Article

Cell Reports

Ceramide Synthase Schlank Is a Transcriptional Regulator Adapting Gene Expression to Energy Requirements

Graphical Abstract

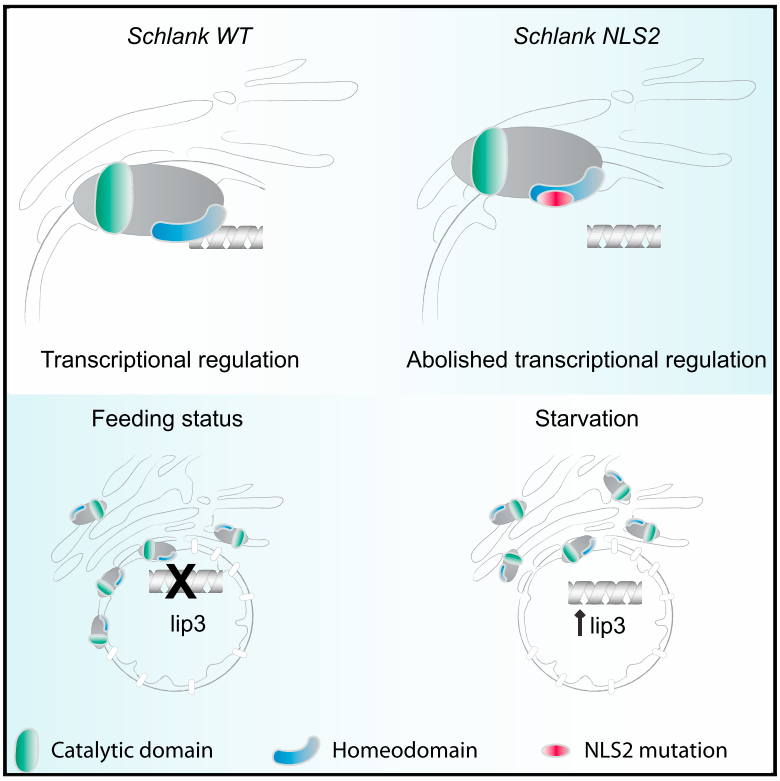

Highlights

- *Drosophila* ceramide synthase (CerS) Schlank binds DNA via its homeodomain
- CerS Schlank has a double role as an enzyme and a transcriptional regulator
- Mutation in the homeodomain of Schlank results in deregulated lipid homeostasis

Authors

Mariangela Sociale, Anna-Lena Wulf, Bernadette Breiden, ..., Joachim Schultze, Konrad Sandhoff, Reinhard Bauer

Correspondence

r.bauer@uni-bonn.de

In Brief

Sociale et al. report that the ceramide synthase Schlank, a multiple transmembrane protein containing a catalytic lag1p motif and a homeodomain, can act as a transcriptional regulator.

Sociale et al., 2018, Cell Reports *22*, 967–978
January 23, 2018
https://doi.org/10.1016/j.celrep.2017.12.090

CellPress

Cell Reports
Article

Ceramide Synthase Schlank Is a Transcriptional Regulator Adapting Gene Expression to Energy Requirements

Mariangela Sociale,[1,5] Anna-Lena Wulf,[1,5] Bernadette Breiden,[2] Kathrin Klee,[3] Melanie Thielisch,[1] Franka Eckardt,[1] Julia Sellin,[1] Margret H. Bülow,[1] Sinah Löbbert,[1] Nadine Weinstock,[1] André Voelzmann,[4] Joachim Schultze,[3] Konrad Sandhoff,[2] and Reinhard Bauer[1,6,*]

[1]LIMES-Institute, Unit Development, Genetics and Molecular Physiology, Department for Molecular Developmental Biology, University of Bonn, Carl-Troll-Strasse 31, 53115 Bonn, Germany
[2]LIMES-Institute, Unit Membrane Biology & Lipid Biochemistry, c/o Kekulé Institute of Organic Chemistry and Biochemistry, University of Bonn, Gerhard-Domagk-Strasse 1, 53121 Bonn, Germany
[3]LIMES-Institute, Unit Molecular Immune and Cell Biology, Department of Genomics and Immunoregulation, University of Bonn, Carl-Troll-Strasse 31, 53115 Bonn, Germany
[4]Faculty of Life Sciences, University of Manchester, Michael Smith Building, Oxford Road, M13 9PT, Manchester, UK
[5]These authors contributed equally
[6]Lead Contact
*Correspondence: r.bauer@uni-bonn.de
https://doi.org/10.1016/j.celrep.2017.12.090

SUMMARY

Maintenance of metabolic homeostasis requires adaption of gene regulation to the cellular energy state via transcriptional regulators. Here, we identify a role of ceramide synthase (CerS) Schlank, a multiple transmembrane protein containing a catalytic lag1p motif and a homeodomain, which is poorly studied in CerSs, as a transcriptional regulator. ChIP experiments show that it binds promoter regions of lipases *lipase3* and *magro* via its homeodomain. Mutation of nuclear localization site 2 (NLS2) within the homeodomain leads to loss of DNA binding and deregulated gene expression, and NLS2 mutants can no longer adjust the transcriptional response to changing lipid levels. This mechanism is conserved in mammalian CerS2 and emphasizes the importance of the CerS protein rather than ceramide synthesis. This study demonstrates a double role of CerS Schlank as an enzyme and a transcriptional regulator, sensing lipid levels and transducing the information to the level of gene expression.

INTRODUCTION

Organismal energy homeostasis (EHS) is a highly coordinated process. Energy is stored in the form of triacylglycerides (TAGs) in specialized organs such as mammalian adipose tissue or the fat body (fb) of flies (Arrese and Wells, 1997; Rosen and Spiegelman, 2006). Coordinating lipid storage and mobilization during times of energy abundance or deprivation (Zechner et al., 2005; Baumbach et al., 2014) is crucial for EHS. Lipases are key enzymes that regulate TAG metabolism. Misregulation of lipase function may lead to loss of the balance of lipolysis and lipogenesis and may have severe consequences leading to metabolic abnormalities such as obesity, lipodystrophy syndromes, and changes in the insulin signaling pathway (ILS).

Recent studies suggested a link between the ILS, ceramides (Cers), and obesity-associated metabolic dysfunction (Reali et al., 2017; Turpin et al., 2014). It was shown that C16-ceramide accumulation alters the ILS. Yet a complete molecular understanding is currently lacking.

Ceramides are generated by linking coenzyme A-activated fatty acids (FAs) of varying length to a sphingoid long-chain base via N-acylation. *De novo* ceramide generation is catalyzed by CerSs, the key enzymes in sphingolipid metabolism (Hannun and Obeid, 2008). CerSs and their product ceramides have been linked to many physiological and pathophysiological processes, such as neurodegeneration (Ferlazzo et al., 2016), obesity-associated metabolic dysfunction (Kolak et al., 2007), inflammatory pathways, and insulin resistance (Schilling et al., 2013; Holland et al., 2011).

The CerS gene family comprises a group of highly conserved transmembrane (TM) proteins in eukaryotes (Park and Pewzner-Jung, 2013; Voelzmann and Bauer, 2010). The number of CerSs between species is quite variable. Whereas mammals express six CerS orthologs, *Drosophila* encodes for only one CerS gene, called *schlank* (Park and Pewzner-Jung, 2013; Bauer et al., 2009). Each CerS family member shares a conserved lag1p motif within a TLC (Tram-Lag1-CLN8) domain essential for CerS activity (Spassieva et al., 2006). All vertebrate and insect CerS orthologs except CerS1 variants contain a homeodomain embedded in a protein carrying multiple TM regions (Voelzmann and Bauer, 2010). However, its function is poorly understood.

Homeodomain proteins are important transcription factors (TFs) that regulate diverse biological functions (de Mendoza et al., 2013). Disruption of homeobox genes is linked to many disorders and diseases (Quinonez and Innis 2014; Purkayastha and Roy 2015). Recently, genome-wide association studies identified a missense coding SNP (E115A) within the homeobox of

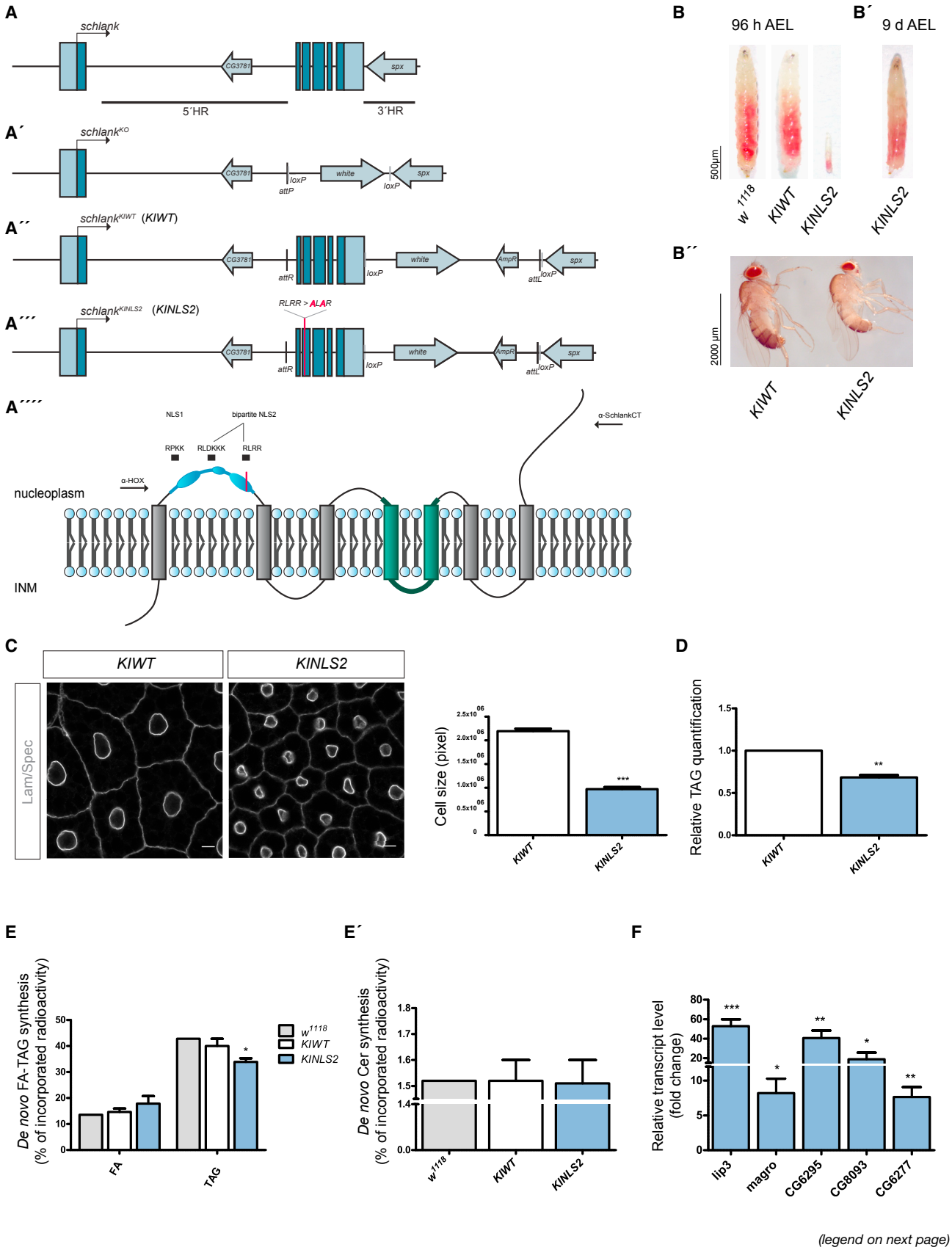

(legend on next page)

the CerS2 gene that might be associated with indicators of insulin resistance or impaired glucose tolerance (Raichur et al., 2014).

We previously identified a nuclear pool of the entire CerS Schlank at the inner nuclear membrane (INM) besides the described CerS pool on the endoplasmic reticulum (ER) (Voelzmann et al., 2016). Rescue experiments in *schlank*^{G0061} mutants, which have reduced TAG levels and upregulated lipases (*lipase3*; *lip3*) (Bauer et al., 2009, 2010), showed that the nuclear function of Schlank is required for the regulation of lipid homeostasis (LHS) via its homeodomain. Expression of enzymatically deficient full-length Schlank (H215D mutation in the lag1p motif) or of nuclear Schlank variants containing the intact homeodomain without the lag1p motif in *schlank*^{G0061} mutant background rescued the TAG phenotype. In contrast, a variant with a point mutation in part of the atypical bipartite-like nuclear localization site 2 (NLS2) motif within the homeodomain did not rescue (Voelzmann et al., 2016). Information on whether the homeodomain of this enzyme has a function *in vivo* is missing by the lack of an animal model.

Maintaining LHS requires monitoring of the lipids status and adapting metabolism through the regulation of gene expression accordingly. This task is often performed by proteins combining the ability of TFs and the sensing of the energy status either alone or in combination with other factors (Varga et al., 2011). TFs, sterol regulatory element binding protein (SREBP; Rawson 2003), a membrane-bound TF, and peroxisome proliferator-activated receptor (PPAR; Varga et al., 2011), a member of the nuclear receptor hormone superfamily, respond to changing fat concentrations, thereby coordinating the genomic response to altered metabolic conditions to promote either fat storage or catabolism.

Currently, no molecular mechanism is known by which CerS enzymes might link changing fat concentrations to altered transcriptional response.

This study demonstrates an unprecedented function of the enzyme CerS Schlank as a nuclear TF. We find that Schlank binds DNA and directly regulates transcription. This mechanism is conserved in mammalian CerSs. Upon treatment with fatty acids, nuclear Schlank is increased while starvation leads to diminished nuclear Schlank. Loss of the ability to bind DNA leads to deregulation of a number of genes, as shown by qRT-PCR, and disrupts the transcriptional adaption of target genes to changing fat conditions.

In sum, our data indicate that CerS Schlank has a double role as CerS and transcriptional regulator, thereby identifying a mechanism by which information about the availability of fat is directly transduced into regulated gene expression.

RESULTS

In Vivo Function of CerS Schlank Homeodomain in Body Fat Metabolism

To study the homeodomain function *in vivo*, we used a homologous recombination and phage ΦC31 integrase-based genomic engineering approach. First, we generated *schlank*^{KO} (knockout [KO]) lines (Figures 1A and S1A), which were verified by molecular and genetic tests (Figures S1A–S1D; Supplemental Information). Next, target constructs containing the deleted genomic DNA (gDNA) of *schlank* without (*pGE-attB schlank*^{KIWT}; knockin [KI] wild-type [*KIWT*]) and with a point mutation in part of the atypical bipartite-like NLS2 (*pGE-attB schlank*^{KINLS2} [*KINLS2*]) lying within the third helix of the homeodomain (Figure 1A′′′′) were reintegrated into the native *schlank* locus in the *schlank*$^{KO\ founder\ line}$ (Figures 1A′′, 1A′′′, and S1A), restoring the target locus (Figures S1A and S1B). qRT-PCR analyses revealed that the transcript levels of *schlank* and of genes within or close to its genomic locus were similar in *schlank KIWT*, *schlank KINLS2*, and w^{1118} control animals (Figures S1E and S1F), confirming expression of reintegrated gDNA. Notably, *KIWT* flies were indistinguishable from wild-type (WT) flies (w^{1118}). Strikingly, *KINLS2* animals revealed a slimness phenotype (Figures 1B) similar to *schlank*^{G0061} mutants (Bauer et al., 2009). However, in *schlank*^{G0061} mutants, transcript levels and *de novo* CerS activity were severely reduced. In summary, molecular and phenotypic analysis of the engineered *schlank* alleles validated our genomic engineering approach. Importantly, reintegration of *schlank* gDNA completely reversed the mutant phenotype.

Figure 1. Characterization of Engineered Schlank Alleles

(A–A′′′′) Generation of *KINLS2* mutants.

(A) Schematic of the *schlank* locus before targeting and (A′) after targeting (*schlank*^{KO}).

(A′′) Diagram showing the reintegration of the deleted WT gDNA to generate *KIWT*.

(A′′′) Diagram showing the reintegration of the deleted gDNA with mutations of two arginines (R) into alanine (RLRR → ALAR) to generate *KINLS2*.

(A′′′′) Putative Schlank protein topology at the INM. Gray boxes indicate transmembrane (TM) domains, blue marks the homeodomain and its helices, and yellow the lag1p motif. Monopartite-like NLS1 (RPKK, aa 78–81) and atypical bipartite-like NLS2 (RLDKKK-X19RLRR, aa 97–125) are depicted above the homeodomain. Arrows indicate the region toward which the antibodies are directed, and the magenta bar within helix 3 indicates the NLS2 mutation.

(B–B′′) KINLS2 mutants show growth defects. Food intake was controlled by feeding red-colored yeast.

(B) Larval growth of w^{1118} (left) and *KIWT* (middle) controls compared with *KINLS2* larvae (right) 96 hr (h) and (B′) 9 days (d) after egg laying.

(B′′) Two-day-old *KIWT* and *KINLS2* adults.

(C) Cell size is reduced in fb cells of *KINLS2* mutants. Lamin Dm0 (Lam; gray) and Spectrin (Spec; gray) were used to mark the INM and the cell membrane. Scale bars represent 20 μm.

(D) Triacylglycerides (TAG) in *KINLS2* L3 larvae are reduced. Relative TAG content was normalized to dry weight.

(E and E′) Metabolic labeling experiment in larvae using [1-^{14}C]-acetic acid to determine TAG and *de novo* ceramide generation. Equal amounts of radioactivity were applied to TLC plates, and percentage of the incorporated label was quantified. Biosynthesis of ceramide in *KINLS2* mutants showed no difference in comparison with w^{1118} and *KIWT* controls (E′), whereas (E) generation of TAG is reduced in *KINLS2* mutants.

(F) Transcript levels of tested lipases in *KINLS2* L3 larvae were quantified using qRT-PCR (*KIWT* was used as control).

Error bars indicate SEM. *$p < 0.05$, **$p < 0.01$, and ***$p < 0.001$.

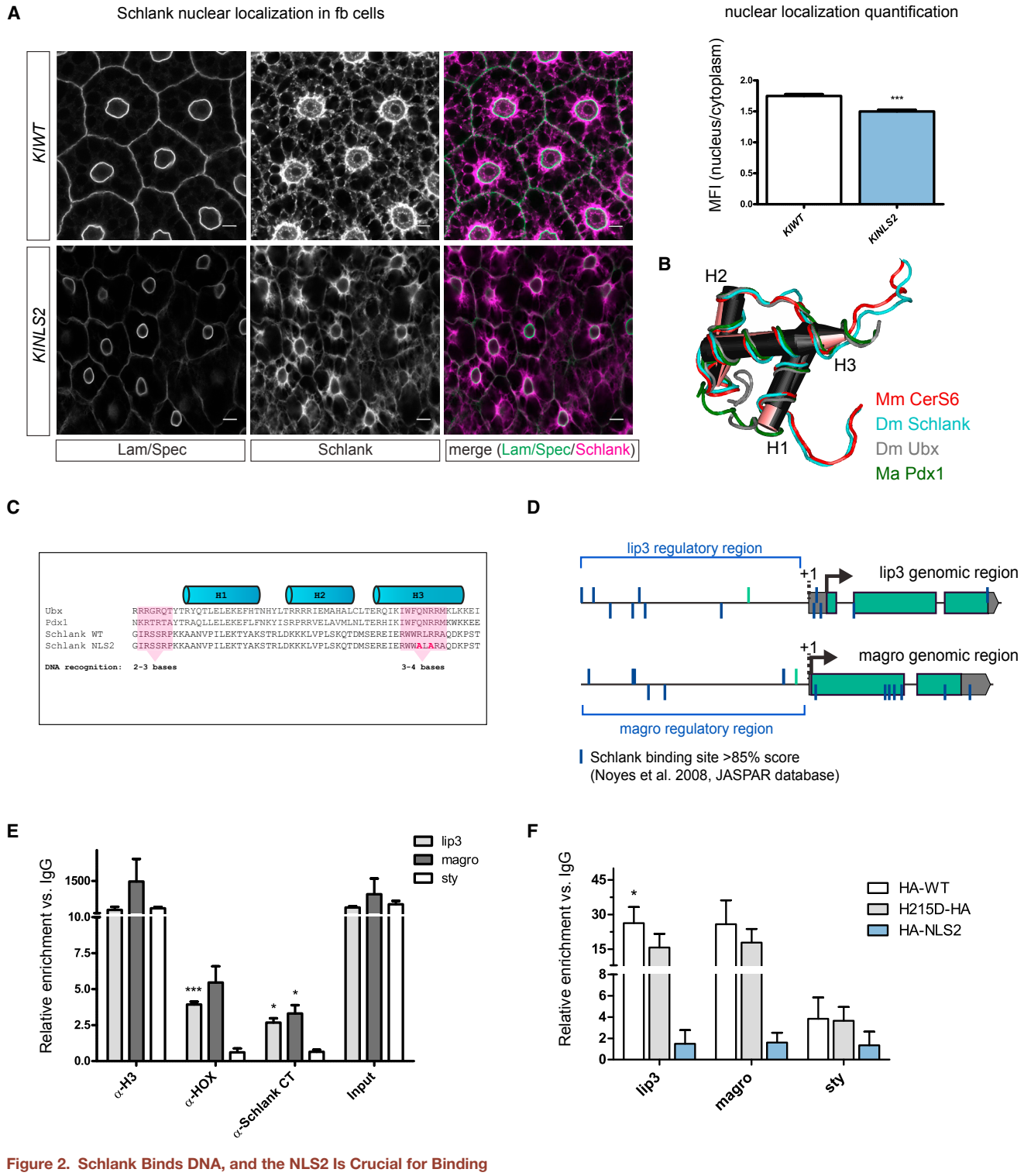

Figure 2. Schlank Binds DNA, and the NLS2 Is Crucial for Binding

(A) Relative mean fluorescence intensities (MFIs) of nucleus/cytoplasm, determined in fb cells of *KINLS2* and *KIWT* (L3) larvae using α-Schlank CT antibodies (magenta). Cells were stained for Lamin Dm0 and Spectrin (green) and DAPI (blue). Scale bars represent 10 μm.

(B) A Schlank SWISS-MODEL follows the 3D structures of CerS6 and classical homeodomains Ubx or Pdx 1. H, helix, Drosophila melanogaster (Dm), Mus musculus (Mm), Mesocricetus auratus (Ma).

(C) Homeodomain alignment showing a DNA recognition motif within the first and third helixes highlighted in pink.

(D) Schematic of the *lip3* and *magro* genomic locus with putative Schlank binding sites, selected according to the putative Schlank binding consensus sequence (>85% matrix identity). Schlank sites depicted in green are within regions that were amplified by qRT-PCR on ChIP material.

(legend continued on next page)

Thus, we conclude that phenotypes of *KINLS2* mutants are exclusively linked to the Schlank homeodomain function thereby presenting an animal model to study its function *in vivo*.

Further analysis of *KINLS2* mutants showed that they are delayed in growth, and about 35% reached the pupa stage at about 9–11 days after egg laying, of which some (10%) eclosed as small-sized adults of normal proportion (Figures 1B″ and S2A) showing locomotion deficits.

Because growth occurs almost exclusively during the larval stage, we focused on *KINLS2* larvae for further analyses, and we used morphological criteria to ensure that WT and mutant animals of the same developmental stage were selected (wandering third-instar larvae [L3]).

We found that *KINLS2* larvae reaching the L3 stage were almost similar in size as control larvae, but they appeared slimmer. Furthermore, the size of fb cells in *KINLS2* larvae was smaller, and TAG levels were significantly reduced, consistent with the observed phenotype (Figures 1C and 1D).

To rule out any contribution to the phenotype by any impairment of the enzymatic function, we performed a metabolic labeling experiment on larvae fed for 18 hr with the radiolabeled lipid precursor [1-^{14}C]- acetic acid. In line with the overall loss of TAG in *KINLS2* larvae, the experiment showed that the *de novo* synthesis of TAG was reduced, accompanied by slightly increased *de novo* fatty acid synthesis (Figure 1E). Notably, there was no difference in CerS activity, resulting in an unchanged *de novo* ceramide synthesis between *KINLS2* and control w^{1118} or *KIWT* larvae (Figure 1E′). Therefore, and because there were no differences in transcript levels of tested genes between w^{1118} or *KIWT* animals (Figures S1E), we henceforth refer only to *KIWT* as control.

In sum, the data from our animal model demonstrate an essential *in vivo* function of the Schlank homeodomain in the regulation of body fat metabolism and growth.

Lipases Are Chronically Upregulated in *KINLS2* Mutants

Growth during developmental phases requires substantial amounts of lipids for expansion of cellular membranes and energy supply. Organisms access energy stored in the form of TAGs in the fb via the tightly coordinated action of lipases (lipolysis). TAG levels were reduced in *KINLS2* larvae, although they feed. Therefore, we tested for the expression of *lip3*, which was strongly upregulated in $schlank^{G0061}$ mutants and repressed upon overexpression of *schlank* (Bauer et al., 2009). qRT-PCR revealed an increase of *lip3* transcript in *KINLS2* larvae (Figure 1F). We next examined transcript levels of several lipases, which have been recently studied in the context of LHS: *CG6295* (Palanker et al., 2009), *CG6277* and *CG8093* (Nirala et al., 2013), and *magro* (Sieber and Thummel, 2009). The expression of these lipases was also increased in fed *KINLS2* animals (Figure 1F). The upregulation of all these lipases except *magro* upon starvation was reported before in association with reduced TAG levels (Palanker et al., 2009), which is in agreement with the observed TAG reduction in *KINLS2* larvae. Starvation response genes other than *lip3*, such as insulin receptor (*InR*), *thor*, and *bmm*, were not transcriptionally upregulated in *KINLS2* larvae. However, their expression was induced upon starvation (Figures S2B and S2C), indicating a normal starvation response.

These data suggest that transcript levels of these lipases are chronically deregulated in *KINLS2* mutants regardless of energy status.

The CerS Enzyme Schlank Is a Transcriptional Regulator

Because mutation of the Schlank homeodomain affects transcription, we sought to identify a mechanism by which Schlank mediates transcriptional control. We previously reported that the NLS2 within the Schlank homeodomain is functional and that nuclear Schlank is required for body fat homeostasis (FHS) (Voelzmann et al., 2016). Therefore, we asked whether nuclear localization might be impaired in *KINLS2* animals. We used specific antibodies (Voelzmann et al., 2016) to determine the distribution of nuclear versus cytoplasmic Schlank in fb cells of *KINLS2* and *KIWT* animals. Nuclear Schlank staining of fb cells of *KINLS2* larvae was moderately (~15%) but significantly reduced compared with *KIWT* larvae (Figure 2A). However, this reduction leaving considerable nuclear Schlank would not explain the whole extent of the loss of nuclear Schlank function, which is demonstrated by the severe phenotypes observed in *KINLS2* mutant animals.

Mostly, homeodomain proteins act as TFs and regulators of differential gene expression programs in development (Gehring et al., 1994). However, a previous study questioned whether the homeodomain might act as a sequence-specific TF (Mesika et al., 2007). Our modeling of the Schlank homeodomain revealed that the folding corresponds to the common DNA-binding architecture (Figure 2B) of homeodomain TFs such as Ultrabithorax (Ubx) or Pancreatic and duodenal homeobox 1 (Pdx 1). In addition, a bioinformatics scan of the promoter region of lipases *lip3* and *magro* identified sites (Figure 2D) conforming to a supposed Schlank binding consensus, determined in a study analyzing the pure homeodomain DNA-binding specificities of putative *Drosophila* homeodomains (Noyes et al., 2008).

Thus, we wondered whether CerS Schlank might bind DNA directly and act as a transcriptional regulator. To test this, we performed chromatin immunoprecipitation (ChIP) experiments on endogenous Schlank from *Drosophila* Schneider cells (S2 cells). We prepared chromatin and pulled down Schlank-associated DNA with anti-Schlank antibodies directed against the C terminus (α-Schlank CT; Voelzmann et al., 2016) or an antibody against the homeodomain (α-HOX; Figures 1A′′′′ and S2D). As positive and negative controls, we performed immunoprecipitations (IPs) using anti-histone α-H3 and α-IgG antibodies,

(E) Schlank binds *lip3* and *magro* promoter regions. Quantification by qRT-PCR of ChIP material from S2 cell extract using α-HOX, α-Schlank CT, IgG, and α-H3 antibodies as negative and positive controls, respectively. Promoter regions assayed were those of *lip3*, *magro*, and *sty* (negative control). Expression was normalized to the relative expression of IgG-ChIP (n = 3).

(F) NLS2 mutation prevents ChIP of *lip3* and *magro* promoter regions. Quantification by qRT-PCR of ChIP material from S2 cell extract transfected with *HA-WT*, *H215D-HA* (n = 3), and *HA-NLS2* using α-HA antibody (n = 4). Promoter regions assayed were those of *lip3*, *magro*, and *sty* (negative control).

Error bars indicate SEM.

respectively. Interestingly, qRT-PCR on the ChIP material revealed that promoter regions of lipases *lip3* and *magro* (containing putative Schlank binding consensus sites with scores >90% and 95%, respectively; Figure 2D) were strongly enriched in both Schlank ChIPs compared with an unrelated genomic region of *sprouty* (*sty*), which was used as negative control (Figure 2E). These data indicate that the TM protein CerS Schlank binds the *lip3* and *magro* promoter region, identifying *lip3* and *magro* as direct Schlank targets.

Mutation of the NLS2 Motif Impairs DNA Binding and Thereby Transcriptional Regulation

Our results shown above support a model whereby Schlank DNA binding is required to mediate a negative regulatory effect on lipase transcription. The NLS2 mutations (RLRR to ALAR), which affects part of the atypical bipartite-like NLS2 (RLDKKK-X19RLRR, amino acids [aa] 97–125) overlap with the putative DNA-binding region of helix three of the homeodomain. Moreover, it contains a defined key residue (arginine) for sequence-specific DNA binding (Bürglin and Affolter, 2016) at position 50 (RLRR) of the homeodomain (Figure 2C). Therefore, we tested whether this Schlank variant might no longer bind to DNA. To this end, we used *HAWT (UAS-HAschlank,* N-terminal [NT] HA tag), ceramide synthesis-deficient Schlank with an H215D mutation *H215D-HA* (*UASschlankH215D-HA*, C-terminal [CT] HA tag), and *HA-NLS2 (UAS-HAschlankNLS2*, NT HA tag). We expressed these variants in S2 cells and performed ChIP. qRT-PCR on the immunoprecipitated material revealed that promoter regions of *lip3* and *magro* were enriched in the HA-ChIP from an HA-WT and H215D extract compared with the genomic region of the negative controls *sty* or microRNA mir-278 (Figures 2F and S2G). In contrast, promoter regions of *lip3* and *magro* were not enriched in the HA-ChIP from the HA-NLS2 variant (Figure 2F). These data indicate that the Schlank NLS2 variant is not able to bind to DNA, while an intact lag1p motif is not required for DNA binding.

To further validate the quality of our ChIP data and to prove that Schlank has a potential as transcriptional regulator, we performed luciferase reporter assays. We therefore cloned a 1.7 kb *lip3* upstream regulatory region (nucleotide position −1665 to −75 with respect to the transcription start; Figure 2D) into a firefly luciferase reporter. Our previous experiments suggested a repression of *lip3* transcription upon overexpression of Schlank WT or a ceramide synthesis-deficient H215D variant (Bauer et al., 2009; Voelzmann et al., 2016). Indeed, cotransfection of S2 cells with full-length Schlank WT or H215D variants along with the *lip3* reporter resulted in a strong repression of *lip3* reporter activity (Figure 3A). Increased or no change of *lip3* reporter activity upon cotransfection with *schlank RNAi* or of an unrelated TF, AP-2, confirmed the efficacy and specificity of the *lip3* reporter (Figures S2H and S2I). These data demonstrate that the *lip3* region used in our reporter assay serves as a Schlank-responsive *cis*-regulatory promoter element.

To test whether transcriptional regulation of the *lip3* activity depends on DNA binding, we transfected S2 cells with *lip3* reporter and *HA-NLS2*, which cannot bind DNA. Of note, the NLS2 variant failed to suppress *lip3* reporter activity (Figure 3A). Thus, DNA binding of Schlank mediated via the homeodomain is required for transcriptional regulation.

To further confirm our results *in vivo*, we expressed *HA-WT* or *WT-HA* (*UASschlank-HA*, CT HA tag), *H215D-myc* (*UASschlankH215D-myc*, CT myc tag), and *HA-NLS2* Schlank variants in *KINLS2* mutants, using a specific fb driver (*cg*Gal4; Pastor-Pareja and Xu, 2011). Transcription of *lip3* was strongly reduced upon expression of the *HA-WT* or *H215D* variant. In contrast, expressing the *HA-NLS2* variant in *KINLS2* mutants did not repress *lip3* expression (Figure 3B), demonstrating that the DNA-binding capacity of Schlank is required to transcriptionally control body FHS.

The data presented above provide mechanistic evidence that CerS Schlank controls body FHS by binding DNA via the intact homeodomain, thereby acting as transcriptional regulator, whereas the catalytic activity is not required for the observed effects. In sum, these data suggest that CerS Schlank has a double function as CerS enzyme and as a transcriptional regulator.

CerSs Are Conserved Transcriptional Regulators

Whereas *Drosophila* encodes for only one CerS, mammals express six CerS orthologs, and all except CerS1 contain a homeodomain. Moreover, the homeodomain of mammalian CerSs except for CerS3 contain NLS2-like motifs (Voelzmann et al., 2016), suggesting a nuclear role similar to CerS Schlank.

We therefore asked whether other homeodomain containing CerSs might also be able to directly regulate transcription. To this end, we transfected S2 cells with the *lip3* reporter and a murine WT *HA-CerS2* (*UAS-HA-CerS2*, NT HA tag) or a catalytically dead H215D variant *CerS2-H215D-HA* (*UASCerS2-H215D-HA*, CT HA tag) CerS2 homolog. Interestingly, expression of both the WT and H215D CerS2 variants resulted in a repression of the *lip3* reporter activity (Figure 3C) comparable with the repression seen when overexpressing the corresponding Schlank versions (Figure 3A). If the homeodomain of CerS2, namely, the NLS2 within, is needed for transcriptional regulation, then luciferase activity should not be reduced upon overexpression. Indeed, the *CerS2-NLS2-HA (UASCerS2-NLS2-HA*, CT HA tag) variant could not suppress *lip3* reporter activity (Figure 3C), suggesting that the NLS2 is required for transcription. Thus, the mammalian enzyme CerS2 appears to have the ability to regulate transcription at the promoter level.

Next we examined whether CerS2 has also a role as transcriptional regulator *in vivo*. Therefore, we expressed *HA-CerS2*, *CerS2-H215D-HA*, and *CerS2-NLS2-HA* variants in the fb of *KINLS2* mutants. Transcription of *lip3* was repressed upon expression of *HA-CerS2 or CerS2-H215D-HA* in *KINLS2* mutants. Strikingly, expression of a CerS2 NLS2 variant did not repress *lip3* expression (Figure 3D). These data strongly suggest that the homeodomain function as transcriptional regulator might be conserved among CerS enzymes.

Schlank Is Required for Adapted Transcriptional Regulation

Under which conditions would Schlank modulate gene expression as transcriptional regulator? We observed deregulated lipases, reduced *de novo* TAG, and increased *de novo* fatty acid synthesis (Figures 1E and 1F). Fatty acids are important as

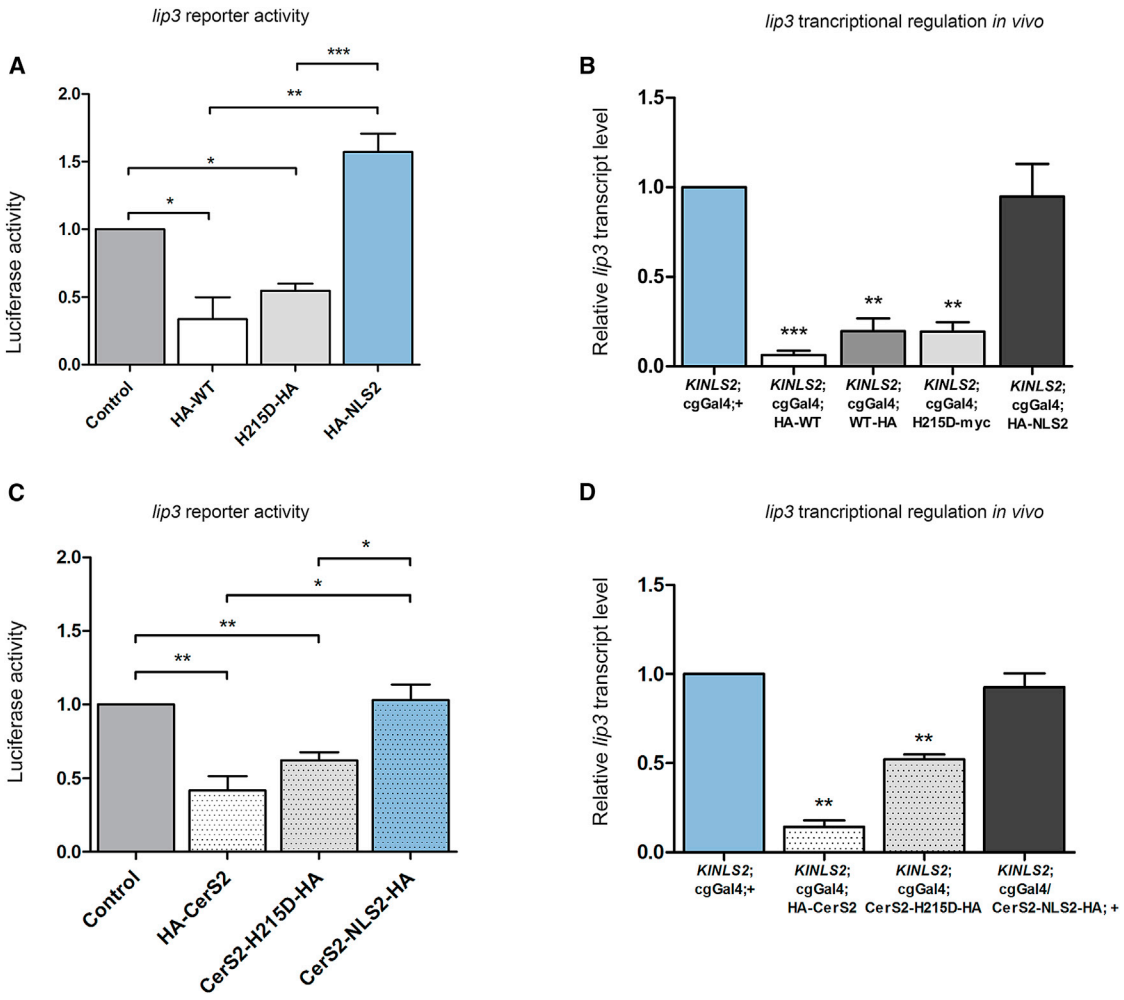

Figure 3. *lip3* Is a Direct Schlank Target, Repressed upon Overexpression of an Intact *Schlank* and Mouse *CerS2* Variant

(A) A 1.7 kb *lip3* enhancer was introduced into a luciferase reporter plasmid containing an actin basal promoter and firefly luciferase (*lip3* reporter). Relative luciferase induction upon expression of *HA-WT*, *H215D-HA*, or *HA-NLS2* is indicated, normalized to *Renilla* luciferase control transfection. The control bar is in reference to luciferase activity upon *UAS-GFP* control expression (n = 3).

(B) Transcript levels of *lip3* in L3 *KINLS2* mutant larvae upon expression of *HA-WT* or *WT-HA*, *H215D-myc*, or of a Schlank NLS2 variant (*HA-NLS2*) under control of the *cgGal4* driver line. Transcript levels were determined using qRT-PCR (n = 3).

(C) Relative luciferase induction upon expression of either *HA-CerS2*, *CerS2-H215D-HA*, or *CerS2-NLS2-HA* (n = 3).

(D) Transcript levels of *lip3* in *KINLS2* mutant larvae upon expression of *HA-CerS2* or *CerS2-NLS2-HA* using the *cgGal4* driver line. *KINLS2* larvae carrying the *cgGal4* driver line but not expressing Schlank variants were used as control. Transcript levels were determined using qRT-PCR (n = 3).

Error bars indicate SEM.

structural components, fuel molecules, and signaling mediators leading to the regulation of gene expression (Varga et al., 2011). The availability of fatty acids is also important for *de novo* ceramide synthesis, raising the question of whether fatty acids might have an effect on Schlank-mediated transcription regulation. To test this, we treated fb and gut from *KINLS2* and *KIWT* larvae with fatty acids of different chain lengths *ex vivo*. Noteworthy, in WT controls, *ex vivo* fatty acid treatment led to suppression of *lip3* and *magro* transcription (Figure 4A). In contrast, in samples obtained from *KINLS2* animals, *ex vivo* fatty acid treatment did not lead to a suppression of *lip3* and *magro* (Figure 4B).

To rule out an unspecific effect on transcriptional regulation by the general gain of energy through increased β-oxidation upon fatty acid treatment, we blocked β-oxidation with etomoxir (a carnitine palmitoyltransferase [cpt] inhibitor) using the same experimental setup. This did not affect the results (Figures S3A and S3B). Thus, Schlank adapts transcriptional regulation according to fatty acid status.

These data are in line with the observed localization of Schlank upon starvation and under fed conditions in S2 cells. Nuclear localization of the endogenous and tagged Schlank decreased with increasing starvation time (Figures 4C, S3C, and S4), suggesting that Schlank is thereby removed from DNA. Importantly, a reduction of nuclear Schlank upon starvation was also observed in starving larvae, further confirming our data *in vivo* (Figure S3E). Upon fatty acid treatment, however, nuclear accumulation of

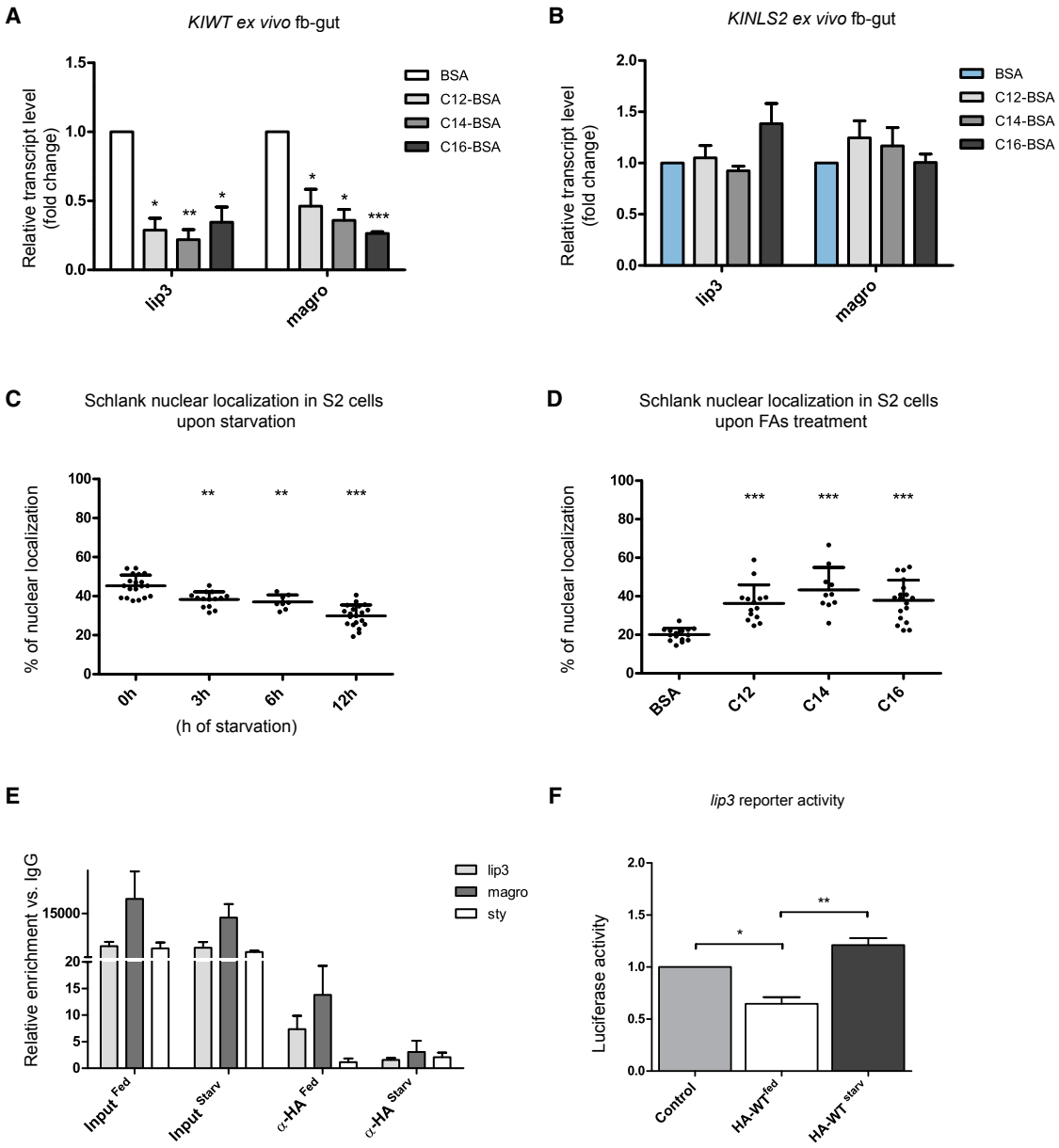

Figure 4. *Ex Vivo* Assay of Dissected Fat Bodies and Gut from *schlank*^{KIWT} and *schlank*^{KINLS2} Larvae and Localization of Schlank in S2 Cells

(A and B) Incubation (6 hr) of e*x vivo* cultures in sugar-free Ringer's solution supplemented with saturated fatty acids of different chain length (C12, C14, and C16) coupled to BSA. BSA only was used as control.

(A) qRT-PCR on *KIWT* fat bodies/guts.

(B) qRT-PCR on *KINLS2* fat bodies/guts. Error bars indicate SEM.

(C and D) Nuclear localization of Schlank determined in S2 cells after starvation (serum deprivation) (C) and supplementation with fatty acids (D). Schlank staining was done with α-schlank CT antibodies. The ratio of colocalized Schlank and DAPI versus cytoplasmic Schlank was quantified and plotted as percentage of nuclear Schlank.

(E) Quantification by qRT-PCR of ChIP material from S2 cell extract transfected with *HA-WT*, which then were fed or starved for 6 hr, using α-HA antibody (n = 3).

(F) Relative luciferase induction upon expression of either *HA-WT* in fed and starved S2 cells (n = 3).

Error bars indicate SEM.

Schlank was increased (Figures 4D and S3D). To further support the model that Schlank DNA binding shifts during fed and starved states, we expressed *HA-WT* Schlank in S2 cells, which then were either fed or starved, and performed ChIP. qRT-PCR on the immunoprecipitated material revealed that *lip3* and *magro* were enriched in the HA-ChIP from fed S2 cells compared with the negative control. However, upon starvation, *lip3* and *magro* promoter regions were no longer enriched in the HA-ChIP (Figure 4E).

Consistent with our ChIP data, we found that luciferase reporter activity was not suppressed upon starvation of S2 cells that had been transfected with the *lip3* reporter (Figure 4F).

In sum, these data support the idea that Schlank may sense fatty acid levels and adjust transcriptional regulation according to the fatty acid status, thereby acting as transcriptional regulator.

DISCUSSION

Our results provide a molecular mechanism by which the enzyme CerS Schlank, a multiple TM protein, for which we previously identified a nuclear pool at the INM (Voelzmann et al., 2016), transduces the cellular energy state into adapted gene expression, thereby acting as transcriptional regulator via its homeodomain. All CerSs contain a catalytic lag1p motif required for ceramide synthesis and a homeodomain, which is conserved in many species (Figure S5; Voelzmann and Bauer, 2010). Its role in development or LHS is not known, because of the lack of animal models, and remains a matter of debate.

In this study, we discovered an *in vivo* function of the Schlank homeodomain in the regulation of body fat metabolism and growth. *KINLS2* mutants carrying a mutation in part of the NLS2 motif lying within the homeodomain show reduced TAG levels, a delay of larval development, and chronically upregulated lipase expression regardless of the feeding status (Figures 1D, 1F, S2A, and S2C). In contrast to previous observed *lipase* and TAG phenotypes in *schlank*^{G0061} mutants, transcript levels and *de novo* CerS activity were not affected in our engineered *schlank* NLS2 allele (Figures S1E and 1E′). Hence, the role in LHS and the phenotypes detected can be exclusively assigned to the homeodomain function, which was unresolved until now.

Furthermore, we found reduced nuclear Schlank staining in fb cells of *KINLS2* larvae (Figure 2A). This might be in part an explanation for the observed phenotypes and is in agreement with recent data showing that the import of CerS Schlank into the nucleus requires the intact NLSs within its homeodomain (Voelzmann et al., 2016). However, functional analysis of the NLS sites was done on the pure homeodomain only, not being embedded in a protein carrying multiple TM regions. This may explain why nuclear Schlank staining in *KINLS2* animals is not severely decreased. In addition, the NLS1 motif at the NT part of the homeodomain is still intact, and only part of the bipartite NLS2 motif is mutated. *In vivo*, for efficient exclusion from the nucleus, deletion of NLS1 or of both NLS motifs may be required. This leaves the questions of how Schlank exerts its nuclear function and how it is affected in NLS2 mutants.

In general, homeodomains fold into a stable three-helix bundle preceded by a flexible NT arm. Positioning of a single "recognition" helix in the major groove and the NT arm in the minor groove can establish interactions with a 5–7 bp DNA binding site (Wolberger, 1996). Previous investigators doubted that the homeodomains of CerSs can act as TFs because of many differences from the homeodomain consensus sequence and argued that they may instead have a modifying role in modulating CerS activity (Mesika et al., 2007; Levy and Futerman, 2010).

A key finding of this study is the identification of CerS Schlank as a transcriptional regulator. Our ChIP data suggest that a pool of the entire Schlank is nuclear and directly binds to promoter regions of the *lip3* and *magro* target genes via its homeodomain (Figures 2E and 2F). We found that mutation of the NLS2 motif within the homeodomain of Schlank, which coincides with the DNA recognition stretch in classical homeodomains and contains a residue for sequence-specific DNA binding (Bürglin and Affolter, 2016) at position 50 (RLRR; Figures 1A′′′′ and 2C), leads to the loss of DNA-binding capacity, abolishing the transcriptional control exerted by Schlank (Figures 2F and 3A). The H215D mutation within the lag1p motif, which is outside the homeodomain, did not affect its DNA-binding capacity (Figures 2F) and demonstrates that enzymatic activity is not required for the effects observed. Furthermore, although the NLS2 mutation affects nuclear localization only moderately, it abolishes DNA binding.

Notably, repression of upregulated *lip3* in *KINLS2* mutants requires an intact NLS2. In contrast, Schlank with mutated NLS2 could not repress the upregulation of *lip3* (Figures 3A and 3B).

Similarly, mutation of the NLS2-like motif in the murine CerS2 led to a loss of transcriptional control and loss of the ability to repress the upregulation of *lip3* in *KINLS2* mutants (Figures 3C and 3D). This indicates that the NLS2 motif is also functional in mammals. Mammals express six different forms of CerSs, and all except CerS1 contain a homeodomain. All homeodomain-containing CerSs except CerS3 have NLS2-like motifs. Our data suggest that CerSs harboring NLS2-like motifs within the homeodomain might have a dual function as CerS enzymes and as transcriptional regulators. CerSs would thereby represent a putative group of transcriptional regulators.

This role is further corroborated by the observation that in *peroxisome 19* (*pex19*) mutants, showing the major hallmarks of the multiform pathologic symptoms of peroxisomal biogenesis disorders of Zellweger syndrome, nuclear Schlank is reduced and lipolysis upregulated. Expression of a nuclear Schlank variant repressed lipolysis and rescued *pex 19* mutants to adulthood (Bülow et al., 2017).

Why use two functions in one protein? Cells need to coordinate gene expression and metabolic state. Metabolism and gene regulation are usually conducted by different classes of proteins.

However, there are examples of metabolic enzymes, such as glyceraldehyde-3-phosphate dehydrogenase and inosine monophosphate dehydrogenase (Zheng et al., 2003; Kozhevnikova et al., 2012), that perform double duty as transcriptional regulators.

Here we show that Schlank adjusts transcriptional regulation, which requires binding of Schlank to DNA via its intact homeodomain, according to energy status, which is also reflected by the fact that Schlank DNA binding shifts during fed and starved states (Figure 4E). NLS2 mutants were no longer able to respond to changing fatty acid levels (Figure 4B). This mechanistic model is consistent with the phenotypes we observed in *KINLS2* animals, which can no longer uphold LHS (Figures 1D and 1F).

Interestingly, the TFs PPAR and SREBP, either as receptor molecules or by interacting with other molecules, sense changing fatty acid conditions and respond as TFs (Desvergne et al., 2006).

Ceramide generation via the *de novo* pathway requires activated fatty acids at two steps: for the condensation of serine

and acyl-CoA by serine-palmitoyl-CoA transferase and for N-acylation of the sphingoid base by coenzyme A-activated fatty acids (Futerman and Hannun, 2004). All CerSs contain a TLC domain, a conserved lipid-sensing domain (Winter and Ponting, 2002), which also determines acyl chain specificity of CerSs (Tidhar et al., 2012). Thus, like PPAR and SREBP, CerS Schlank might sense fatty acid status and transduce the signal by regulating gene expression via its homeodomain. Alternatively, as suggested for SREBP (Dobrosotskaya et al., 2002), Schlank might be required to monitor cell membrane lipid composition and to adjust lipid synthesis accordingly. Of note, the anchoring of Schlank in the membrane is apparently important, as the pure homeodomain of Schlank, which is exclusively nuclear (Voelzmann et al., 2016), was not able to rescue the *lip3* phenotype when it was expressed in *schlank* mutants (Figure S2L). A very recent publication supports the concept of a dual role of CerS in metabolism and transcription (Mendelson et al., 2017). Mutations in the NLS2-like site of the zebrafish CerS2b homeodomain similar to our NLS2 mutations (Voelzmann et al., 2016) abolished the ability to respond to changing sphingosine levels properly.

Future studies will be needed to reveal how CerS Schlank can sense fatty acid levels or metabolites and whether it acts alone or together with other partners to comply with the double function as an enzyme and a transcriptional regulator.

Together, our data suggest a mechanism by which CerS might perform a double role as an enzyme and a transcriptional regulator sensing lipid levels and transducing the information to the level of gene expression. We found that Schlank can bind to DNA via its homeodomain, suggesting a role as a transcriptional regulator. Previous work provided valuable data on the regulatory aspects of CerS biology on the basis of the enzyme activity and the ceramides produced. Our data put the CerS protein rather than ceramide synthesis into focus.

Finally, most CerSs have, in addition to the catalytic lag1p motif, a homeodomain, suggesting the intriguing possibility that CerSs might act to some extent as transcriptional regulators.

EXPERIMENTAL PROCEDURES

Schlank Genomic Engineering, Fly Strains, and Larvae Selection

Schlank knockout flies were generated by homologous recombination as described (Huang et al., 2008). Primers and detailed procedures are described in the Supplemental Information.

The following fly stocks were obtained from the Bloomington Stock Centre: w^{1118}; P{*cg-GAL4.A*}2 (#7011) and w^{1118}; and Tb1 (#42220), Df(1)dx81, w*/Dp(1;Y)dx+1/C(1)M5 (#5281). pP{*UAS-schlank NTHA*}, pP{*UAS-schlank CTHA*}, pP{*UAS-CerS2*} (Bauer et al., 2009), pP{*UAS-GFP*}, and pP{*UAS-schlank^{NLS2}*} (Voelzmann et al., 2016) were described earlier. pP{*UAS CerS2NLS2HA*} and pP{*UAS-schlank-Hox*} were generated by P element transformation (Rubin and Spradling 1982) into w^{1118} flies. Phenotypic analysis of *Schlank* alleles and rescue experiments were done as previously described (Bauer et al., 2009; Voelzmann et al., 2016). Morphological criteria were used to ensure that WT and mutant animals of the same developmental stage were selected (wandering L3).

Cloning and Plasmids

CerS2-NLS2-HA (NLS2 mutation: RRRR to ALAR), *CerS2-H215D-HA*, or *schlankH215D-HA* was inserted into pP{UAST} to produce pP{*UASCerS2-NLS2-HA*}, pP{*UASCerS2-H215D-HA*}, and pP{*UAS schlankH215D-HA*}. p*UAS-GFP*-schlank-aa 64–138 (Voelzmann et al., 2016) was used to produce pP{*UAS-schlank-Hox*} transgenic flies. pP{*UAS-schlank NTHA*} and pP{*UAS-HA-CerS2*}, pP{*UASschlankH215D*} (Bauer et al., 2009), pP{*UAS-GFP*}, and pP{*UAS-schlank^{NLS2}*} (Voelzmann et al., 2016) were described earlier.

The luciferase reporter plasmid contains a 1.7 kb upstream regulatory region of *schlank* cloned into pAc5.1 plasmid upstream of a firefly luciferase reporter gene. Primers used are listed in Table S2.

Cell Culture and Luciferase Assays

Drosophila Schneider cells (S2) were grown in Schneider's medium supplemented with 10% heat-inactivated fetal bovine serum and 1% penicillin/streptomycin (Sigma-Aldrich, USA). Transfection was done 12 hr after plating S2 cells (Effectene; QIAGEN) according to the manufacturer's instruction. Starvation and fatty acid treatment were done in Serum Free Optimem with or without BSA-fatty acids for indicated times. Luciferase assays were performed 48 hr after transfection of the corresponding plasmids with the Dual-Luciferase Reporter Assay System (Promega) according the manufacturer's protocol. Activity was determined using a MicroLumat*Plus* LB 96V luminometer (Berthold Technology). Each experiment was repeated three times and is the average of the reading of three different transfected wells. Antibody staining on S2 cells was performed 48 hr after transfection of S2 cells.

TAG Assay

Organismal fat content (total glycerides) was quantified using a coupled colorimetric assay. The lyophilized samples were weighed, and the dry weight was used to normalize TAG amount. The measurements were carried on as previously described (Tennessen et al., 2014).

Metabolic Labeling of Lipids of Larvae

TAG, fatty acid, and CerS activity was determined by measuring *de novo* TAG, fatty acid, and ceramide generation after 18 hr labeling of larvae with [1-^{14}C]-acetic acid. For metabolic labeling, larvae were fed with inactivated yeast paste containing [1-^{14}C]-acetic acid (61 Ci/mol) as a C1-precursor for lipids. The procedure was carried on as previously described (Bauer et al., 2009).

Antibody Generation

Polyclonal antiserum (α-HOX antibody) was generated in rabbit (BioGenes, Berlin, Germany) against a Schlank-specific oligopeptide (RSSRPKKAANVPI, aa 75–87) conjugated to LHS (Figure S2D).

Immunohistochemistry

For immunohistochemical staining, we used anti-Schlank-CT from guinea pig or sheep (α-Schlank) 1:50 (Voelzmann and Bauer, 2011), anti-HA (α-HA, rat, 1:100; clone 3F10; Roche); anti-Spectrin (α-Spectrin; mouse, 1:40) Developmental Studies, Hybridoma Bank (DSHB), and mouse anti-Lamin Dm0 (DSHB) 1:100. Tissue or cells were mounted with DAPI Fluoromount-G (SouthernBiotech). The procedure was carried out as previously described (Bauer et al., 2009).

Ex Vivo Culture of Larval fb and Gut

Ex vivo organ culture was performed according the method of Britton and Edgar (1998). In brief, L3 were opened and incubated in glucose-free Ringer's solution (120 mM NaCl, 4 mM KCl, 2 mM $CaCl_2$, 4 mM $MgCl_2$, and 5 mM HEPES) supplemented with different BSA-conjugated fatty acids (C12, C14, and C16) to a final concentration of 200 μM for 6 hr at 4°C. BSA was used as control. In parallel, etomoxir was added (200 μM). Following incubation, larvae were washed in PBS, and fat bodies and gut were dissected and frozen in TRIzol (Invitrogen).

RNA Extraction and qRT-PCR

Isolation of total RNA was done in TRIzol. cDNA was transcribed using the QuantiTect Kit (QIAGEN). qRT-PCR was performed in a reaction mix containing cDNA template, primers, and iQ SYBR Green Supermix (Bio-Rad). The experiments were performed in an iQ5 RT-PCR Detection System (Bio-Rad). *Ribosomal protein L32* (*rp49*) was used as a reference gene.

ChIP

ChIP was performed as previously described (Andresini et al., 2016). Briefly, S2 cells were crosslinked with formaldehyde. The nuclei were subsequently sonicated to yield DNA fragments of about 500 bp and immunoprecipitated with the indicated antibodies. Crosslinking was reversed, DNA was extracted

using phenol/chloroform, and 1 μl of immunoprecipitated DNA was used for qRT-PCR analysis. Expanded protocol is provided in the Supplemental Information.

Quantification of Nuclear Schlank

S2 cells were imaged for Schlank (α-Schlank-CT, endogenous) or HA (α-HA; expression of *UAS-schlank NTHA* [*HA-WT*]) and DAPI fluorescence. The nuclear area was defined as DAPI and cytoplasm as total Schlank signal minus nuclear area. The mean fluorescence intensity (MFI) ratio of Schlank to DAPI of nuclear versus cytoplasmic area per cell was determined and quantified using the ImageJ "Intensity Ratio Nuclei Cytoplasm Tool" and plotted as MFI (nucleus/cytoplasm). For fb cells, the nuclear area was defined as DAPI/Lamin Dm0 stained region. The cytoplasmic area was defined as Spectrin area minus nuclear area. The MFI ratio of Schlank fluorescence of nuclear versus cytoplasmic area per cell was determined. For size determination, cells in a comparable confocal plane were compared using DAPI staining, and cell area was defined by Spectrin and outlined using the "Hand" tool. ImageJ software was used for each quantification.

Bioinformatics and Statistical Analysis

Depiction of 3D Protein Data Bank (PDB) structures and phylogenetic analysis data are detailed in the Supplemental Information.

Significance was tested using a two-tailed heteroscedastic Student's t test (Microsoft Excel) with at least three independent biological replicates (n), with the Mann-Whitney U test or with one-way ANOVA as indicated (GraphPad Prism) (*$p < 0.005$, **$p < 0.01$, and ***$p < 0.001$).

SUPPLEMENTAL INFORMATION

Supplemental Information includes Supplemental Experimental Procedures, five figures, and two tables and can be found with this article online at https://doi.org/10.1016/j.celrep.2017.12.090.

ACKNOWLEDGMENTS

We wish to thank D. Peters and NingNing Liu for cloning the donor plasmid and the pGE-attB integration constructs, respectively. We thank Hannes Maib for PCR analysis verifying Schlank knockout lines, C. Schwarzkopf and B. Syllwashi for their support in survival analysis and size determination, and Ikram Arahouan for her help with rescue experiments. We also thank M. Pankratz and T. Lang for critical reading of the manuscript and M. Hoch for his continuous support. This work was supported by the SFB 645 (grants to R.B., J. Schultze, and K.S.) and TRR83 (K.S.). J. Schultze is a member of excellence cluster ImmunoSensation.

AUTHOR CONTRIBUTIONS

Conceptualization, M.S. and R.B.; Methodology, M.S. and A.-L.W.; Validation, M.S. and R.B.; Formal Analysis, M.S. and A.V.; Investigation, M.S., A.-L.W., B.B., M.T., F.E., J. Sellin, M.H.B., S.L., N.W., A.V., and R.B.; Data Curation, K.K.; Writing – Original Draft, R.B.; Writing – Review & Editing, R.B., M.S., A.V., B.B., and K.S.; Visualization, M.S.; Supervision and Project Administration, R.B.; Funding Acquisition, R.B., K.S., and J. Schultze.

DECLARATION OF INTERESTS

The authors declare no competing interests.

Received: August 2, 2017
Revised: November 10, 2017
Accepted: December 25, 2017
Published: January 23, 2018

REFERENCES

Andresini, O., Ciotti, A., Rossi, M.N., Battistelli, C., Carbone, M., and Maione, R. (2016). A cross-talk between DNA methylation and H3 lysine 9 dimethylation at the KvDMR1 region controls the induction of Cdkn1c in muscle cells. Epigenetics *11*, 791–803.

Arrese, E.L., and Wells, M.A. (1997). Adipokinetic hormone-induced lipolysis in the fat body of an insect, Manduca sexta: synthesis of sn-1,2-diacylglycerols. J. Lipid Res. *38*, 68–76.

Bauer, R. (2010). Towards understanding regulation of energy homeostasis by ceramide synthases. Results Probl. Cell Differ. *52*, 175–181.

Bauer, R., Voelzmann, A., Breiden, B., Schepers, U., Farwanah, H., Hahn, I., Eckardt, F., Sandhoff, K., and Hoch, M. (2009). Schlank, a member of the ceramide synthase family controls growth and body fat in *Drosophila*. EMBO J. *28*, 3706–3716.

Baumbach, J., Hummel, P., Bickmeyer, I., Kowalczyk, K.M., Frank, M., Knorr, K., Hildebrandt, A., Riedel, D., Jäckle, H., and Kühnlein, R.P. (2014). A *Drosophila in vivo* screen identifies store-operated calcium entry as a key regulator of adiposity. Cell Metab. *19*, 331–343.

Britton, J.S., and Edgar, B.A. (1998). Environmental control of the cell cycle in *Drosophila*: nutrition activates mitotic and endoreplicative cells by distinct mechanisms. Development *125*, 2149–2158.

Bülow, M.H., Wingen, C., Senyilmaz, D., Gosejacob, D., Sociale, M., Bauer, R., Schulze, H., Sandhoff, K., Teleman, A.A., Hoch, M., and Sellin, J. (2017). Unbalanced lipolysis results in lipotoxicity and mitochondrial damage in peroxisome-deficient Pex19 mutants. Mol. Biol. Cell. Publsihed online December 27, 2017. https://doi.org/10.1091/mbc.E17-08-0535.

Bürglin, T.R., and Affolter, M. (2016). Homeodomain proteins: an update. Chromosoma *125*, 497–521.

de Mendoza, A., Sebé-Pedrós, A., Šestak, M.S., Matejcic, M., Torruella, G., Domazet-Loso, T., and Ruiz-Trillo, I. (2013). Transcription factor evolution in eukaryotes and the assembly of the regulatory toolkit in multicellular lineages. Proc. Natl. Acad. Sci. U S A *110*, E4858–E4866.

Desvergne, B., Michalik, L., and Wahli, W. (2006). Transcriptional regulation of metabolism. Physiol. Rev. *86*, 465–514.

Dobrosotskaya, I.Y., Seegmiller, A.C., Brown, M.S., Goldstein, J.L., and Rawson, R.B. (2002). Regulation of SREBP processing and membrane lipid production by phospholipids in *Drosophila*. Science *296*, 879–883.

Ferlazzo, E., Striano, P., Italiano, D., Calarese, T., Gasparini, S., Vanni, N., Fruscione, F., Genton, P., and Zara, F. (2016). Autosomal recessive progressive myoclonus epilepsy due to impaired ceramide synthesis. Epileptic Disord. *18*, 120–127.

Futerman, A.H., and Hannun, Y.A. (2004). The complex life of simple sphingolipids. EMBO Rep. *5*, 777–782.

Gehring, W.J., Affolter, M., and Bürglin, T. (1994). Homeodomain proteins. Annu. Rev. Biochem. *63*, 487–526.

Hannun, Y.A., and Obeid, L.M. (2008). Principles of bioactive lipid signalling: lessons from sphingolipids. Nat. Rev. Mol. Cell Biol. *9*, 139–150.

Holland, W.L., Bikman, B.T., Wang, L.-P., Yuguang, G., Sargent, K.M., Bulchand, S., Knotts, T.A., Shui, G., Clegg, D.J., Wenk, M.R., et al. (2011). Lipid-induced insulin resistance mediated by the proinflammatory receptor TLR4 requires saturated fatty acid-induced ceramide biosynthesis in mice. J. Clin. Invest. *121*, 1858–1870.

Huang, J., Zhou, W., Watson, A.M., Jan, Y.-N., and Hong, Y. (2008). Efficient ends-out gene targeting in *Drosophila*. Genetics *180*, 703–707.

Kolak, M., Westerbacka, J., Velagapudi, V.R., Wågsäter, D., Yetukuri, L., Makkonen, J., Rissanen, A., Häkkinen, A.-M., Lindell, M., Bergholm, R., et al. (2007). Adipose tissue inflammation and increased ceramide content characterize subjects with high liver fat content independent of obesity. Diabetes *56*, 1960–1968.

Kozhevnikova, E.N., van der Knaap, J.A., Pindyurin, A.V., Ozgur, Z., van Ijcken, W.F.J., Moshkin, Y.M., and Verrijzer, C.P. (2012). Metabolic enzyme IMPDH is also a transcription factor regulated by cellular state. Mol. Cell *47*, 133–139.

Levy, M., and Futerman, A.H. (2010). Mammalian ceramide synthases. IUBMB Life *62*, 347–356.

Mendelson, K., Pandey, S., Hisano, Y., Carellini, F., Das, B.C., Hla, T., and Evans, T. (2017). The ceramide synthase 2b gene mediates genomic sensing and regulation of sphingosine levels during zebrafish embryogenesis. eLife *6*, 6.

Mesika, A., Ben-Dor, S., Laviad, E.L., and Futerman, A.H. (2007). A new functional motif in Hox domain-containing ceramide synthases: identification of a novel region flanking the Hox and TLC domains essential for activity. J. Biol. Chem. *282*, 27366–27373.

Nirala, N.K., Rahman, M., Walls, S.M., Singh, A., Zhu, L.J., Bamba, T., Fukusaki, E., Srideshikan, S.M., Harris, G.L., Ip, Y.T., et al. (2013). Survival response to increased ceramide involves metabolic adaptation through novel regulators of glycolysis and lipolysis. PLoS Genet. *9*, e1003556.

Noyes, M.B., Christensen, R.G., Wakabayashi, A., Stormo, G.D., Brodsky, M.H., and Wolfe, S.A. (2008). Analysis of homeodomain specificities allows the family-wide prediction of preferred recognition sites. Cell *133*, 1277–1289.

Palanker, L., Tennessen, J.M., Lam, G., and Thummel, C.S. (2009). *Drosophila* HNF4 regulates lipid mobilization and beta-oxidation. Cell Metab. *9*, 228–239.

Park, J.-W., and Pewzner-Jung, Y. (2013). Ceramide synthases: reexamining longevity. Handb. Exp. Pharmacol. *215*, 89–107.

Pastor-Pareja, J.C., and Xu, T. (2011). Shaping cells and organs in *Drosophila* by opposing roles of fat body-secreted collagen IV and perlecan. Dev. Cell *21*, 245–256.

Purkayastha, B.P.D., and Roy, J.K. (2015). Cancer cell metabolism and developmental homeodomain/POU domain transcription factors: a connecting link. Cancer Lett. *356* (*2 Pt A*), 315–319.

Quinonez, S.C., and Innis, J.W. (2014). Human HOX gene disorders. Mol. Genet. Metab. *111*, 4–15.

Raichur, S., Wang, S.T., Chan, P.W., Li, Y., Ching, J., Chaurasia, B., Dogra, S., Öhman, M.K., Takeda, K., Sugii, S., et al. (2014). CerS2 haploinsufficiency inhibits β-oxidation and confers susceptibility to diet-induced steatohepatitis and insulin resistance. Cell Metab. *20*, 687–695.

Rawson, R.B. (2003). The SREBP pathway—insights from Insigs and insects. Nat. Rev. Mol. Cell Biol. *4*, 631–640.

Reali, F., Morine, M.J., Kahramanoğulları, O., Raichur, S., Schneider, H.-C., Crowther, D., and Priami, C. (2017). Mechanistic interplay between ceramide and insulin resistance. Sci. Rep. *7*, 41231.

Rosen, E.D., and Spiegelman, B.M. (2006). Adipocytes as regulators of energy balance and glucose homeostasis. Nature *444*, 847–853.

Rubin, G.M., and Spradling, A.C. (1982). Genetic transformation of *Drosophila* with transposable element vectors. Science *218*, 348–353.

Schilling, J.D., Machkovech, H.M., He, L., Sidhu, R., Fujiwara, H., Weber, K., Ory, D.S., and Schaffer, J.E. (2013). Palmitate and lipopolysaccharide trigger synergistic ceramide production in primary macrophages. J. Biol. Chem. *288*, 2923–2932.

Sieber, M.H., and Thummel, C.S. (2009). The DHR96 nuclear receptor controls triacylglycerol homeostasis in *Drosophila*. Cell Metab. *10*, 481–490.

Spassieva, S., Seo, J.-G., Jiang, J.C., Bielawski, J., Alvarez-Vasquez, F., Jazwinski, S.M., Hannun, Y.A., and Obeid, L.M. (2006). Necessary role for the Lag1p motif in (dihydro)ceramide synthase activity. J. Biol. Chem. *281*, 33931–33938.

Tennessen, J.M., Barry, W.E., Cox, J., and Thummel, C.S. (2014). Methods for studying metabolism in *Drosophila*. Methods *68*, 105–115.

Tidhar, R., Ben-Dor, S., Wang, E., Kelly, S., Merrill, A.H., Jr., and Futerman, A.H. (2012). Acyl chain specificity of ceramide synthases is determined within a region of 150 residues in the Tram-Lag-CLN8 (TLC) domain. J. Biol. Chem. *287*, 3197–3206.

Turpin, S.M., Nicholls, H.T., Willmes, D.M., Mourier, A., Brodesser, S., Wunderlich, C.M., Mauer, J., Xu, E., Hammerschmidt, P., Brönneke, H.S., et al. (2014). Obesity-induced CerS6-dependent C16:0 ceramide production promotes weight gain and glucose intolerance. Cell Metab. *20*, 678–686.

Varga, T., Czimmerer, Z., and Nagy, L. (2011). PPARs are a unique set of fatty acid regulated transcription factors controlling both lipid metabolism and inflammation. Biochim. Biophys. Acta *1812*, 1007–1022.

Voelzmann, A., and Bauer, R. (2010). Ceramide synthases in mammalians, worms, and insects: emerging schemes. Biomol. Concepts *1*, 411–422.

Voelzmann, A., and Bauer, R. (2011). Embryonic expression of *Drosophila* ceramide synthase schlank in developing gut, CNS and PNS. Gene Expr. Patterns *11*, 501–510.

Voelzmann, A., Wulf, A.L., Eckardt, F., Thielisch, M., Brondolin, M., Pesch, Y.Y., Sociale, M., Bauer, R., and Hoch, M. (2016). Nuclear *Drosophila* CerS Schlank regulates lipid homeostasis via the homeodomain, independent of the lag1p motif. FEBS Lett. *590*, 971–981.

Winter, E., and Ponting, C.P. (2002). TRAM, LAG1 and CLN8: members of a novel family of lipid-sensing domains? Trends Biochem. Sci. *27*, 381–383.

Wolberger, C. (1996). Homeodomain interactions. Curr. Opin. Struct. Biol. *6*, 62–68.

Zechner, R., Strauss, J.G., Haemmerle, G., Lass, A., and Zimmermann, R. (2005). Lipolysis: pathway under construction. Curr. Opin. Lipidol. *16*, 333–340.

Zheng, L., Roeder, R.G., and Luo, Y. (2003). S phase activation of the histone H2B promoter by OCA-S, a coactivator complex that contains GAPDH as a key component. Cell *114*, 255–266.